PAPER

Strain effect on intersubband transitions in rolled-up quantum well infrared photodetectors

Strain effect on intersubband transitions in rolled-up quantum well infrared photodetectors*

Han Wang[2], Shilong Li[1], Honglou Zhen[1], Xiaofei Nie[1,2], Gaoshan Huang[3], Yongfeng Mei[3,†], and Wei Lu[1,†]

[1]National Laboratory for Infrared Physics, Shanghai Institute of Technical Physics, Chinese Academy of Sciences, Shanghai 200083, China
[2]University of Chinese Academy of Sciences, Beijing 100049, China
[3]Department of Materials Science, Fudan University, Shanghai 200433, China

Abstract: Pre-strained nanomembranes with four embedded quantum wells (QWs) are rolled up into three-dimensional (3D) tubular QW infrared photodetectors (QWIPs), which are based on the QW intersubband transition (ISBT). A redshift of ~0.42 meV in photocurrent response spectra is observed and attributed to two strain contributions due to the rolling of the pre-strained nanomembranes. One is the overall strain that mainly leads to a redshift of ~0.5 meV, and the other is the strain gradient which results in a very tiny variation. The blue shift of the photocurrent response spectra with the external bias are also observed as quantum-confined Stark effect (QCSE) in the ISBT.

Key words: quantum well infrared photodetector; rolled-up microtube; strain; Stark effect
DOI: 10.1088/1674-4926/38/5/054006 **PACS:** 61.72.Uj; 73.21.Fg; 62.20.dq

1. Introduction

Functional inorganic nanomembranes with embedded quantum wells (QWs) or self-assembled quantum dots (QDs) have shown the ability to roll up into three-dimensional (3D) micro-/nanoscale tubular structures/devices[1−3]. The embedded quantum entities can manifest themselves as light emitters, so that various optical components based on the 3D microstructures have been demonstrated such as optical microcavities[4−6], lasers[7, 8], and couplers[9]. The strain issue due to the rolling is of interest and has been recently investigated for these optical components[10, 11]. On the other hand, the quantum entities embedded in nanomembranes can be functionalized as on-demand light absorbers for optoelectronics[12]. For instance, 3D tubular infrared photodetectors based on the QW intersubband transition (ISBT) have recently been demonstrated, in which an omnidirectional coupling characteristic has been observed owing to their circular symmetric structure[13]. Hence, the strain effect due to the rolling[11] is expected on these optoelectronic devices. However, so far as we know, there is no report about the strain effect on the performance of such rolled-up tubular optoelectronic devices from planar nanomembranes.

In this letter, we investigate the strain effect on ISBT in rolled-up QW infrared photodetectors (QWIPs). QW-embedded nanomembranes are rolled up as 3D tubular QWIPs and the photocurrent response as the external bias is measured experimentally. Energy shifts of the response spectra in these QWIP devices is analyzed and can be attributed to the variation of strain states. These results can help with not only the further development of the 3D tubular QWIPs, but also the physical understanding of other rolled-up optoelectronic devices.

2. Device fabrication

The 3D tubular QWIP was rolled up from multilayered nanomembranes grown by metal-organic chemical vapor deposition (MOCVD) on GaAs (100) substrate, as sketched in Fig. 1(a). The layered structure of the designed nanomembranes is shown in Fig. 1(b). Starting from the substrate, a 30-nm AlAs sacrificial layer was first grown, and the next layer is a 20-nm $In_{0.2}Al_{0.2}Ga_{0.6}As$ strained layer, followed by a 40-nm GaAs bottom contact layer with an n-doping of 1×10^{18} cm^{-3}. Then, on the 3-nm AlAs corrosion block layer, four QWs composed of a 5.5-nm n-doping (5×10^{17} cm^{-3}) GaAs well and two 30-nm $Al_{0.28}Ga_{0.72}As$ barriers per period were grown. The remaining layers were a 20-nm n-doping (1×10^{18} cm^{-3}) GaAs conductive layer, a 2-nm AlAs corrosion block layer, and a 300-nm n-doping (1×10^{18} cm^{-3}) GaAs top contact layer. In the end, the QW-embedded nanomembrane was rolled up into a microtube when the underneath AlAs sacrificial layer was removed. More details on the fabrication processes of such a rolled-up tubular QWIP can be found in the previous work[13]. Here, an optical image of a 3D tubular QWIP as well as the SEM image of the part of a microtube are shown in Figs. 1(c) and 1(d). In addition, planar QWIP devices with a 45° edge facet were fabricated for comparison, which have the same layered structure of nanomembrane and the same area of active region as those of the tubular devices. These QWIP devices were fixed in a Dewar and operated at around 70 K. Unpolarized

* Project supported by the Natural Science Foundation of China (Nos. 51322201, 61575213), and the Shanghai Municipal Science and Technology Commission (No. 14JC1400200).
† Corresponding author. Email: yfm@fudan.edu.cn, luwei@mail.sitp.ac.cn
Received 26 October 2016, revised manuscript received 3 December 2016

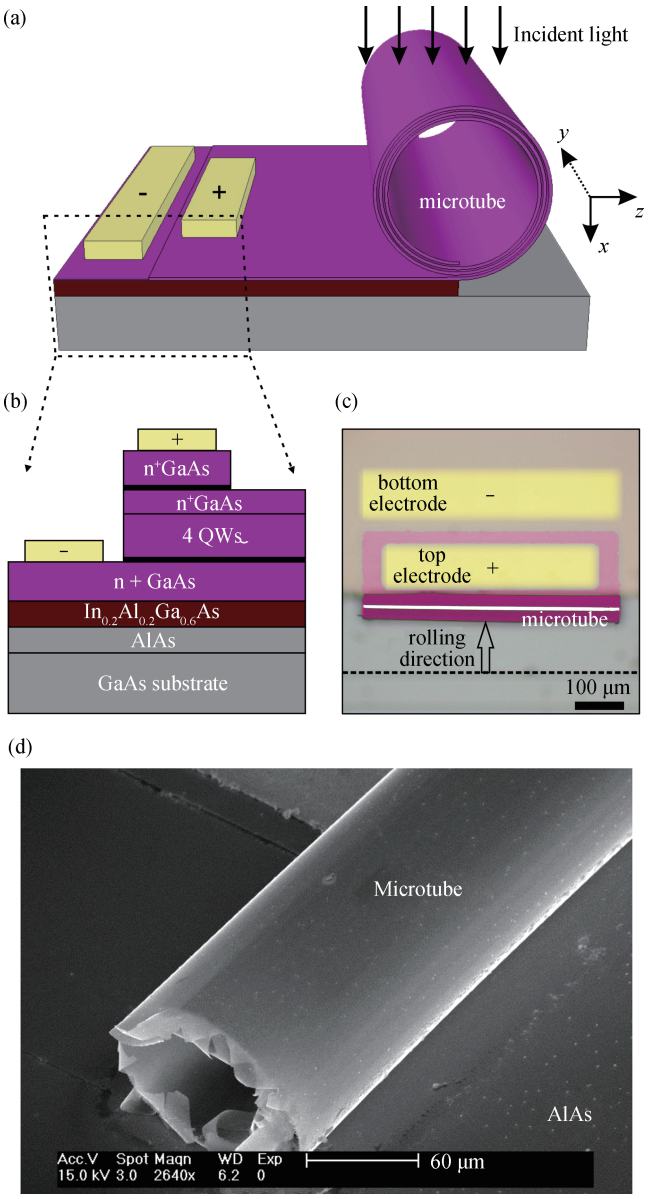

Fig. 1. (Color online) (a) Schematic diagram, (b) layer sequence, (c) optical image of a rolled-up QWIP device, and (d) SEM image of the part of a tubular device.

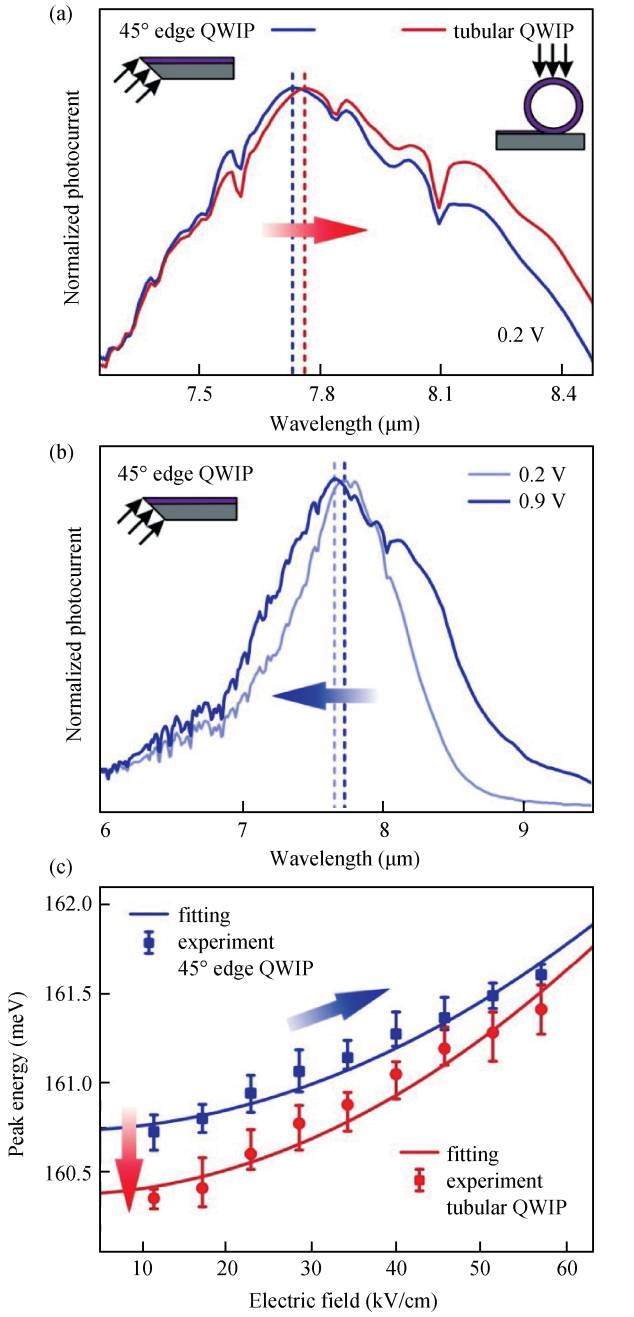

Fig. 2. (Color online) (a) Normalized photocurrent response spectra of the 3D tubular and the corresponding 45° edge-facet QWIPs under a bias of 0.2 V. Schematic drawings of these QWIPs are given in the inset. The red arrow indicates the direction of a redshift. (b) Normalized photocurrent response spectra of the 45° edge-facet QWIPs under biases of 0.2 and 0.9 V, respectively. The blue arrow indicates the direction of a blueshift. (c) Peak energies of these QWIP devices as a function of applied electric field.

infrared light was shone on the top of the 3D tubular devices, as shown in Fig. 1(a) and the right inset in Fig. 2(a), whereas the planar device was illuminated by the incident light on the 45° edge facet, as shown in the left inset in Fig. 2(a). Photocurrent response spectra were measured by a Fourier transform infrared (FTIR) spectrometer (Nicolet 6700).

3. Results and discussion

The normalized photocurrent response spectra of the 3D tubular and the corresponding 45° edge-facet QWIPs under a bias of 0.2 V are shown in Fig. 2(a). About 20-nm redshift for the peak wavelength is observed for the 3D tubular device compared to the planar one. The shift of the peak wavelength results from the strain relaxation for the rolling, and has been observed in optical spectra of the passive rolled-up structures as well[11, 14]. However, none of these works used the QW ISBT, or few of them realized an optoelectronic active device. Hence, the strain-induced shift for the ISBT in rolled-up QWIP devices will be explained in detail later.

3.1. QCSE

Fig. 2(b) shows the normalized photocurrent response spectra of the 45° edge-facet QWIPs under various biases. As can be seen, about 57-nm blueshift for the peak wavelength is

observed as the bias increases from 0.2 to 0.9 V. The blueshift is attributed to the well-known quantum-confined Stark effect (QCSE)[15, 16] in ISBT. The QCSE of the 45° edge-facet QWIP devices is more evident in Fig. 2(c), where the peak energy as a function of the bias is shown and a parabolic relationship between the two physical quantities is clearly visible. According to the second-order perturbation theory of QCSE[17], the Stark energy shift ΔE for a symmetric QW is proportional to the external electric field F^2, i.e.,

$$\Delta E = 2q^2F^2\frac{|z_{12}|^2}{E_2 - E_1} = A_{\text{symm}}F^2, \tag{1}$$

where q is the electron charge, z_{12} is the element of the dipole matrix, and E_1, E_2 are the ground state and the first excited state energy of the QW, respectively. Therefore, the calculated result A_{symm} for our 45° edge-facet QWIP is $\sim 3.2 \times 10^{-4}$ meV·cm^2·kV^{-2}, which is in good agreement with the experiment result $\sim 2.9 \times 10^{-4}$ meV·cm^2·kV^{-2}. As shown in Fig. 2(c), the parabolic QCSE is also observed for the 3D tubular devices, which, however, have a larger value A_{symm} $\sim 3.5 \times 10^{-4}$ meV·cm^2·kV^{-2}. It is the result of lattice relaxation of QWs after the rolling, which leads to the variation in the width of QWs and the shape of conduction-band edges.

3.2. Strain effect on the ISBT

As mentioned above (see Figs. 2(a) and 2(c)), the peak energy of photocurrent response spectra redshifts about 0.42 meV when a planar QW nanomembrane is rolled up into a microtube. The QW nanomembrane is a multilayered structure. The initial strain $\varepsilon_{\text{int\_QW}}$ in the QW region can be simplified as zero since the lattice constants of GaAs and $Al_{0.28}Ga_{0.72}As$ are almost the same. The strain for the rolling is from the strained $In_{0.2}Al_{0.2}Ga_{0.6}As$ layer, where the initial strain $\varepsilon_{\text{int\_InAlGaAs}}$ is about 1.43%. When the pre-strained nanomembrane is bent, the lattice constants and the resultant strain states are altered[18, 19]. The total volumetric strain ε_{QW} in the QW region of the bent nanomembrane can be described by[19]

$$\varepsilon_{\text{QW}}(z) = \varepsilon_{0\_\text{QW}} + \frac{1-2\upsilon}{1-\upsilon}\frac{z}{R}, \tag{2}$$

where υ is the Poisson's ratio, $1/R$ is the curvature, and the coordinate origin is located at the inner surface of the bent nanomembrane. It is seen from Eq. (2) that the volumetric strain ε_{QW} consists of two parts, i.e., the overall strain $\varepsilon_{0\_\text{QW}}$ across the QW region and the strain gradient $[(1-2\upsilon)/(1-\upsilon)](z/R)$. The former is a constant which is not equal to $\varepsilon_{\text{int\_QW}}$ because of the redistribution of strain after the bending/rolling, and the latter is a variable determined by the continuity of lattice. Since the photocurrent response of our devices comes mainly from the ISBT of QWs, only the effect of strain on the conduction band is considered. The energy shift for the conduction-band edge (Gamma band edge) due to the strain relaxation reads[20]

$$E_{\text{C}}^{\text{str}} = a_{\text{C}}\varepsilon_{\text{QW}}(z) = a_{\text{C}}\varepsilon_{0\_\text{QW}} + a_{\text{C}}\frac{1-2\upsilon}{1-\upsilon}\frac{z}{R}, \tag{3}$$

where a_{C} is the deformation potential[21]. It contains two contributions as well: the overall strain potential $a_{\text{C}}\varepsilon_{0\_\text{QW}}$ across the QW region and the strain gradient potential $a_{\text{C}}[(1-2\upsilon)/(1-\upsilon)](z/R)$. The two contributions on the ISBT of QWs are different, and are discussed in the following.

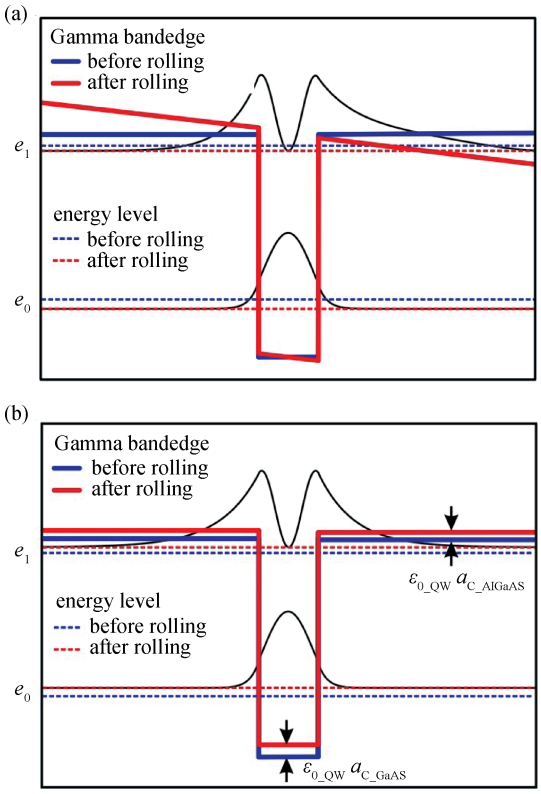

Fig. 3. (Color online) Conduction-band diagrams of a single QW in a planar nanomembrane (blue solid lines, before rolling) and the resultant rolled-up nanomembrane (red solid lines, after rolling) under the effect of (a) the strain gradient potential and (b) the overall strain potential, respectively. The first two energy levels of the intersubband electron are plotted (dashed lines) with the corresponding wave functions (black solid lines).

First of all, the strain gradient potential is a linear function of the coordinate z. As a result, the QW conduction-band edge is tilted, as shown in Fig. 3(a). Since the 30-nm barrier layer is thick enough to prevent coupling between the intersubband electron wave functions confined in the adjacent wells, only a single QW is considered here. Similar to the QCSE in ISBT, the energy shift induced by the strain gradient potential which acts as a perturbation term can also be solved based on the second-order perturbation theory, and is given by

$$\Delta E_{\text{grad}} = 2\left(\frac{a_{\text{C}}}{R}\frac{1-2\upsilon}{1-\upsilon}\right)^2\frac{|z_{12}|^2}{E_2 - E_1}, \tag{4}$$

with the parameters of $a_{\text{C\_GaAs}} = -7.17$ eV[22], $\upsilon = 0.31$[22], and $R = 35\ \mu$m, ΔE_{grad} is about 5×10^{-4} meV for the 3D tubular devices. It is positive, and thus will give rise to a blueshift in the photocurrent response spectrum, which is contrary to the experimental observations. However, it is also too small to be observed and can be ignored. Therefore, the redshift in photocurrent response spectra does not originate from the strain gradient potential.

Now the effect of the overall strain potential $a_{\text{C}}\varepsilon_{0\_\text{QW}}$ on the ISBT of QWs is inspected. Since the QW strain has a linear

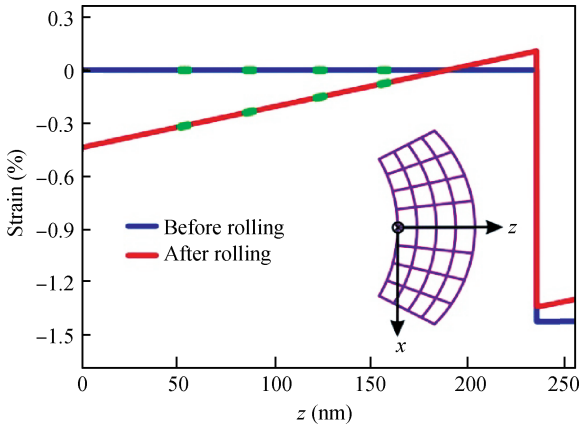

Fig. 4. (Color online) Strain distributions in the QW nanomembranes before (blue solid line) and after (red solid line) the rolling. Green short lines indicate the position of the four wells embedded into the nanomembranes.

relationship with the QW position (see Eq. (2)), the calculated average strain of all four wells in the QW region is equal to that of all five barriers and the overall strain ε_{0_QW} is the averaged strain of the four QWs. The deformation potentials of the well a_{C_GaAs} and the barrier a_{C_AlGaAs} are −7.17 and −6.78 eV[22], respectively. As a result, the conduction-band edge of the well and barrier are shifted differently. As shown in Fig. 3(b), the Gamma band edges of the well and the barrier move respectively $a_{C\_GaAs}\varepsilon_{0\_QW}$ and $a_{C\_AlGaAs}\varepsilon_{0\_QW}$, so that the change in the depth of a QW is $\varepsilon_{0\_QW}(a_{C\_AlGaAs} - a_{C\_GaAs})$. To determine the overall strain ε_{0_QW} and the QW depth, the strain distribution in the QW nanomembrane is calculated and the results are shown in Fig. 4. The overall strain ε_{0_QW} is about −0.18%, which indicates that the QWs are compressed after the rolling. Therefore, the QW depth is reduced about 0.7 meV, which leads to a redshift of ∼0.5 meV for the ISBT by calculating the bound state energy levels in the one-dimensional finite square potential well. In the end, by taking into account the effect of the strain gradient potential as we discussed above, the total energy shift for the 3D tubular devices is about −0.5 meV. It is in accordance with the experimental result of about −0.42 meV. The slight variation could be due to the uniformity of composition and thickness[20, 22]. It is thus concluded that the redshift in photocurrent response spectra of the rolled-up tubular QWIPs is due to the variation in the overall strain potential.

The ISBT energy is shifted since the strain state of QWs varies as a nanomembrane undergoes a structural change from a plane to a 3D microtube. For our 3D tubular QWIPs used here, it is shown that the energy shift due to the overall strain is much larger in the magnitude than that caused by the strain gradient, and the directions of the two energy shifts are opposite. However, these ISBT energy shifts can be altered by varying the size of the microtube and/or the layered structure of the nanomembrane. For example, if the radius of the microtube is reduced to several micrometers[3, 4] and an asymmetric QW is employed, the energy shift caused by the strain gradient could be dominant. Moreover, the overall strain can even lead to a blue shift by engineering the strain distribution.

4. Conclusion

The 3D tubular QWIPs from QW-embedded planar nanomembranes have been fabricated on the basis of the rolled-up nanotechnology. The blueshift in photocurrent response spectra of the rolled-up QWIP devices as the external bias varies has been explained as the QCSE in ISBT. The redshift in the photocurrent spectra as the planar nanomembranes are rolled up into microtubes has been analyzed in detail, and mainly attributed to the change of the overall strain. Our results demonstrate that strain states in nanomembranes can be used for tuning the light absorption of a QWIP device, and for potential applications in QW-based emitters or microtube-based optoelectronic devices.

References

[1] Rogers J A, Lagally M G, Nuzzo R G. Synthesis, assembly and applications of semiconductor nanomembranes. Nature, 2011, 477(7362): 45
[2] Huang G S, Mei Y F. Thinning and shaping solid films into functional and integrative nanomembranes. Adv Mater, 2012, 24(19): 2517
[3] Li X L. Self-rolled-up microtube ring resonators: a review of geometrical and resonant properties. Adv Opt Photonics, 2011, 3(4): 366
[4] Kipp T, Welsch H, Strelow C, et al. Optical modes in semiconductor microtube ring resonators. Phys Rev Lett, 2006, 96(7): 077403
[5] Vicknesh S, Li F, Mi Z. Optical microcavities on Si formed by self-assembled InGaAs/GaAs quantum dot microtubes. Appl Phys Lett, 2009, 94(8): 081101
[6] Ma L, Kiravittaya S, Quiñones V A B, et al. Tuning of optical resonances in asymmetric microtube cavities. Opt Lett, 2011, 36(19): 3840
[7] Bianucci P, Mukherjee S, Dastjerdi M H T, et al. Self-organized InAs/InGaAsP quantum dot tube lasers. Appl Phys Lett, 2012, 101(3): 031104
[8] Dastjerdi M H T, Djavid M, Mi Z. An electrically injected rolled-up semiconductor tube laser. Appl Phys Lett, 2015, 106(2): 021114
[9] Bhowmick S, Heo J, Bhattacharya P. A quantum dot rolled-up microtube directional coupler. Appl Phys Lett, 2012, 101(101): 171111
[10] Mei Y F, Kiravittaya S, Benyoucef M. Optical properties of a wrinkled nanomembrane with embedded quantum well. Nano Lett, 2007, 7(6): 1676
[11] Zhen H L, Huang G S, Kiravittaya S, et al. Light-emitting properties of a strain-tuned microtube containing coupled quantum wells. Appl Phys Lett, 2013, 102(4): 041109
[12] Dastjerdi M H T, Mi Z. Nanoscale rolled-up InAs quantum dot tube photodetector. Electron Lett, 2014, 50(9): 680
[13] Wang H, Zhen H L, Li S L, et al. Self-rolling and light-trapping in flexible quantum well-embedded nanomembranes for wide-angle infrared photodetector. Sci Adv, 2016, 2(8): e1600027
[14] Kubota K, Vaccaro P O, Ohtani N, et al. Photoluminescence of GaAs/AlGaAs micro-tubes containing uniaxially strained quantum wells. Physica E, 2002, 13(2): 313
[15] Harwit A, Harris J S Jr. Observation of Stark shifts in quantum well intersubband transitions. Appl Phys Lett, 1987, 50(11): 685
[16] Miller D A B, Chemla D S, Damen T C. Band-edge electroabsorption in quantum well structures: the quantum-confined Stark effect. Phys Rev Lett, 1984, 53(22): 2173
[17] Rosencher E, Vinter B. Optoelectronics. Cambridge: Cambridge

University Press, 2002
[18] Grundmann M. Nanoscroll formation from strained layer heterostructures. Appl Phys Lett, 2003, 83(12): 2444
[19] Binder R, Gu B, Kwong N H. Quantum-confined strain gradient effect in semiconductor nanomembranes. Phys Rev B, 2014, 90(19): 195208
[20] Cendula P, Kiravittaya S, Schmidt O G. Electronic and optical properties of quantum wells embedded in wrinkled nanomembranes. J Appl Phys, 2011, 111(4): 043105
[21] Walle C G V D. Band lineups and deformation potentials in the model-solid theory. Phys Rev B, 1989, 39(3): 1871
[22] Li E H. Material parameters of InGaAsP and InAlGaAs systems for use in quantum well structures at low and room temperatures. Physica E, 2000, 5(4): 215